DEMONSTRATION OF COPPER:PLA-LIKE NANOCOMPOSITE-BASED DISTRIBUTED BRAGG REFLECTOR GAS SENSOR

[1,2]Zdeněk KRTOUŠ, [1]Pavel SOLAŘ, [3]Oleksandr POLONSKYI, [1,4]Jaroslav KOUSAL

[1]Charles University, Faculty of Mathematics and Physics, Prague, Czech Republic, EU,
jaroslav.kousal@mff.cuni.cz

[2]Polytechnique Montreal, Department of Engineering Physics, Montreal, CA

[3]University of California, Santa Barbara, Department of Chemical Engineering, Santa Barbara (CA), USA

[4]Czech Technical University in Prague, Faculty of Mechanical Engineering, Prague, Czech Republic, EU

https://doi.org/10.37904/nanocon.2024.5003

Abstract

Plasma polymerization, commonly considered a type of plasma-enhanced chemical vapour deposition (PECVD), is a popular method for depositing organic thin films. However, it often produces films with limited molecular complexity due to the necessity to use relatively low molar mass precursors that can be vaporized. To address these limitations, plasma-assisted vapour thermal deposition (PAVTD) was developed. In PAVTD, a solid polymer undergoes thermal degradation (evaporation) in a crucible, producing oligomers with higher molar masses (10^2-10^3 g.mol^{-1}) than typical PECVD precursors. These oligomers are then re-polymerized in RF plasma, allowing PAVTD films to exhibit properties characteristic of classical polymer physics and chemistry, a rarity for plasma polymers. This process enables the precise control of properties such as biodegradability and hydrolyzability, as demonstrated in polylactic acid (PLA)-based films.

PAVTD effectively bridges the gap between classical and plasma polymers. To enhance stability and deposition rates, continuous-PAVTD has been developed using standard FDM 3D printing filaments, achieving deposition rates up to several nanometers per second. This advancement addresses deposition duration and stability issues, making PAVTD a practical tool for studying plasma polymerization. Furthermore, PAVTD can be combined with other vacuum-based thin film deposition techniques like gas aggregation source of nanoparticles (GAS). This capability was demonstrated by fabricating Cu:PLA-like nanocomposite-based distributed Bragg reflector (DBR), where the reproducibility of the deposition rate matters significantly. This reflector was tested as a gas sensor for ethanol vapours, exhibiting strong reflectance peak shifts.

Keywords: Plasma-assisted vapour thermal deposition, gas aggregation source, distributed Bragg reflector, nanocomposite, gas sensor

1. INTRODUCTION

Metal-polymer nanocomposites have diverse applications, like antibacterial films or magnetic films [1-3]. One promising application for metal-dielectric nanocomposites is optical thin films, particularly due to their plasmonic (LSPR) properties [4-8]. Their use ranges from photovoltaic coatings or absorbers to Distributed Bragg Reflectors (DBRs) that can used, e.g. as gas sensors.

DBRs are structures (often fully dielectric) exhibiting band- or peak-like reflectance that are composed of layers with alternating refractive indexes ("low-n" and "high-n"), being thus a kind of so-called 1-D photonic crystals. In the most simple form of DBR the layer thicknesses correspond to quarter-wave interference for the wavelength of the reflection peak. While polymers or oxides are often used for the "low-n" layers, the "high-n" layers can be prepared using nanocomposites. The dielectric:dielectric nanocomposites have a rather limited

range of refractive indexes, requiring a large number of layers in a DBR to be effective. Metallic nanoparticle-based nanocomposites can overcome this limitation. DBRs based on nanocomposites can be fabricated using vacuum-based methods, e.g., Au-Teflon, Ag-PTFE or Au-SiO DBRs [9-12].

In this paper, we demonstrate the fabrication of DBR with nanocomposite films based on nanoparticles prepared using a gas aggregation source (GAS) [13]. As the "low-n" layers and as the matrix for the nanocomposite "high-n" layers, PLA-like plasma polymer deposited using plasma-assisted vapour thermal deposition (PAVTD) was used [14]. The use of the PAVTD was possible due to recent improvements in the technique [15].

One application of nanocomposite-based DBRs is gas sensors [16-21]. Typically, the matrix reacts to the presence of sensed gas vapours. Classical polymers exhibit various kinds of "swelling" that change the structural parameters (layer thicknesses) of the DBR and optical properties of its constituents, especially of the nanocomposite. Plasma polymers are typically too crosslinked to exhibit this behaviour efficiently. PAVTD can prepare plasma polymers that exhibit classical polymer-like behaviour [14]. This enables the use of the DBR prepared with this technique as a gas sensor, as demonstrated in this paper.

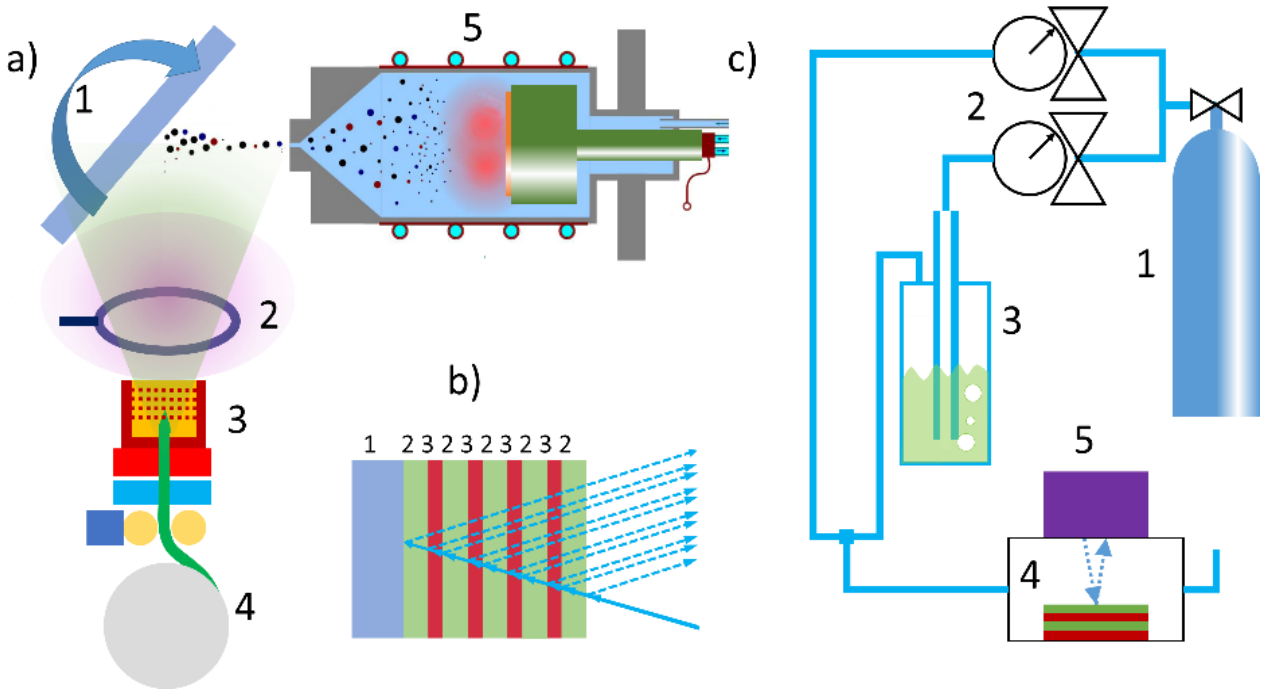

Figure 1 a) Scheme of the deposition setup. 1 – rotatable substrate holder; 2 – RF electrode; 3 – crucible; 4 – polymer (3D printing FDM fiber) storage and feed; 5 – magnetron-based gas aggregation nanoparticle source with copper target b) Scheme of distributed Bragg reflector. 1 – substrate; 2 – low-n film (polymer); 3 – high-n film (metal-polymer nanocomposite) c) Scheme of the gas sensing setup. 1 – gas tank; 2 – flowcontrollers; 3 – bubbler with test chemical; 4 – flow cell with the sample; 5 – UV/VIS spectrophotometer

2. EXPERIMENTAL

First, the distributed Brag reflector (DBR) structure was prepared as a stack of PLA-like layers deposited using plasma-assisted vapour thermal deposition (PAVTD) and nanocomposite films using the same material as a matrix and nanoparticles produced by gas aggregation source (GAS) as a filler.

Second, the DBR structure was checked, and its optical reflectance spectra were measured in an inert and ethanol-containing atmosphere.

2.1 Distributed Bragg reflector preparation

2.1.1 Plasma-assisted vapour thermal deposition

The plasma polymer layers ("low-n" layers of DBR) were deposited using a continuous-PAVTD setup [15] with polylactic acid (PLA) FDM 3D printing fibre ("natural" PLA, Gembird) fed at the rate of 2 g/h. The deposition chamber was fed with argon at the pressure of 0.5 Pa. Above the crucible, plasma discharge at RF (13.56 Mhz) power 5 W was used to induce mild repolymerization in the film (**Figure 1a**).

2.1.2 Nanocomposite layers deposition

The metal-polymer nanocomposite layers ("high-n" layers of DBR) were deposited using the codeposition of PLA-like material (as described in the previous section) with copper nanoparticles produced using GAS with Cu target on DC magnetron, run at the 500 mA current and 70 Pa of argon pressure inside GAS (**Figure 1a**).

2.1.3 Reflector stack deposition

The DBR stack (schematically shown in **Figure 1b**) was deposited on a silicon substrate as 11 alternating layers (6 "low-n", 5 "high-n") by keeping the PAVTD setup running continuously and switching the GAS alternatively. For demonstration purposes, all layers were deposited to a thickness around 100 nm each, the "high-n" nanocomposite layers thinner than the "low-n" polymer layers, as is needed for the DBR structures. The total deposition time of the DBR stack was about 20 minutes.

2.2 DBD stack characterization

The structure of the DBR stack was checked using an SEM microscope (Jeol JSM-7900F) by imaging the crosssection of the DBR on a cut substrate. A UV-VIS-NIR spectrophotometer (Ossila Optical Spectrometer) was used to characterize the DBR reflectance spectra. The DBR was placed into a 3D-printed gas flow cell (internal volume 350 ml) for reflectance measurements (angle of incidence 9°). This flow cell was used to characterize the changes in DBR reflectance spectra with the presence of admixture in the atmosphere. As a model gas, ethanol vapours were chosen. To control the concentration of ethanol in the gas (argon), the gas feed to the flow cell was split into two gas lines: one with pure argon (0.25 liter$_{STP}$/min) and the other going through the bubbler with ethanol (0-1.2 liter$_{STP}$/min), varying the resulting ethanol vapours concentration between 0% and 6% (**Figure 1c**). (Note: The vapour pressure of ethanol at the laboratory temperature was 7.2kPa.)

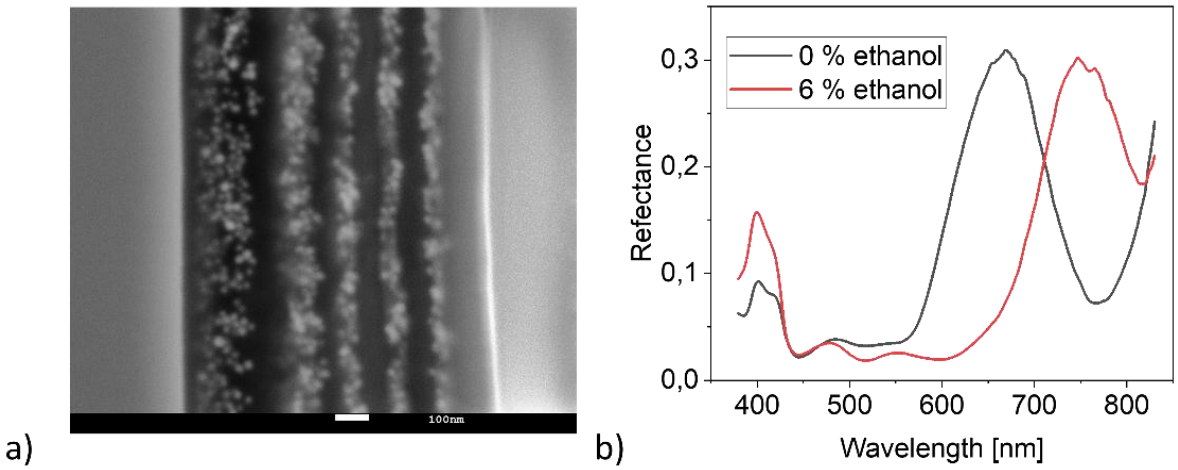

Figure 2 a) SEM image of the crossection of the DBR (substrate side on the left, scale bar 100 nm) (enhanced contrast) b) Reflectance spectra of the DBR in dry argon and Ar+ethanol mixture.

3. RESULTS AND DISCUSSION

3.1 Structure and optical properties

The structure of the deposited DBR, as observed by SEM (**Figure 2a**), was found to be satisfactory, clearly showing the nanocomposite character of the "high-n" layers. The total thickness of the DBR was 880 nm. Due to the visible deviations from purely regular structure, the reflectance was expected to be significantly reduced compared to an ideal DBR. Still, the optical reflectance spectra have clearly shown a Bragg reflectance peak around 660 nm (**Figure 2b**).

3.2 Gas sensing demonstration

With the presence of ethanol vapours in the UV-VIS flow cell, the DBR reflectance peak exhibited a significant spectral shift (**Figure 2b**). For the characterization, the flow cell was repeatedly flushed with pure argon and argon-ethanol mixture. Each ethanol vapour flow took about 100 seconds. The DBR was initially cycled 5 times under an ethanol vapour concentration of 6%. While some relaxation of the DBR reflectance peak shift was observed (the peak shift decreased by about 9 nm), the repeated measurements at the same ethanol concentration (see below) were reproducible within a few nm. Also some relaxation was also observed during each period of ethanol vapour introduction into the cell when the vapour concentration was over ~5.5%.

The sensitivity of the shift of the reflectance peak to the ethanol concentration was then characterized. Time dependences for the peak shift after the introduction of varying concentrations of ethanol into the flow cell are shown in **Figure 3a**. It can be seen that the dynamics of the process are mostly limited by the flow cell volume, especially at the lowest ethanol concentration, where the total gas flow was sufficient to fill the volume of the cell just about 2 times per the filling cycle. In these cases, the real peak shift of the DBR reflectance peak for a corresponding ethanol concentration can be higher than registered. In general, the DBR itself must react under ~30s.

The summary of the sensitivity of the reflectance peak shift is shown in the **Figure 3b**. The peak shift shows nonlinear dependence on the ethanol vapour concentration, reaching a ~100 nm shift for the ethanol concentration of ~6% when the peak moved to about 750 nm. It shall be noted that the DBR stack was neither perfect nor optimized for the maximal physical/chemical interaction with the detected substance.

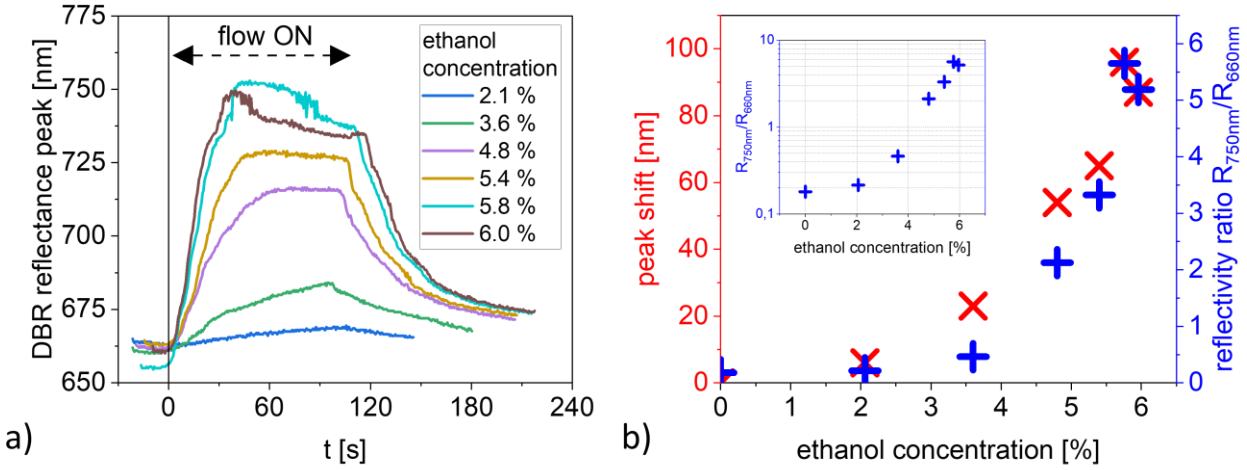

Figure 3 a) Time dependence of the DBR peak position after the introduction of the gas mixture into the flow cell b) Dependence of the peak reflectance on the DBR shift and the dependence of the ratio of reflectances at 660 nm and 750 nm (R_{660nm}/R_{750nm}) on the ethanol concentration (Inset: R_{660nm}/R_{750nm} in semilogarithmic scale).

If some gas sensors are to be based on this kind of DBR stack, instead of full UV-VIS reflectance measurement, two spectral lines reflectance ratio measurement would be much simpler. Selecting the spectral lines of 660 nm and 750 nm (corresponding to measured extremes of reflectance peak position), the R_{750nm}/R_{660nm} reflectance ratio is also shown in **Figure 3b**. Above ~2% ethanol concentration in the atmosphere, the dependence of this ratio on ethanol concentration is almost exponential (**Figure 3b**, inset).

The high peak shift attainable with this DBR as a sensor can be attributed to the reversible swelling of the plasma polymer component of the DBR structure, stretching the thickness of the DBR itself by ~15%. While such significant swelling by solvent adsorption was observed on PAVTD-deposited films [14], it is untypical for common densely crosslinked plasma polymers.

4. CONCLUSIONS

In this paper, the preparation of Cu:PLA-like nanocomposite-based distributed Bragg reflector was demonstrated. The continuous-PAVTD technique is shown to be controllable on the level permitting the preparation of nontrivial optical multilayer stacks and combinable with other vacuum-based deposition techniques, such as GAS, as in this case.

The resulting DBR reflector shows the DBR reflectance peak, limited mostly by the imperfections in the deposition process. Such a DBR stack was then used as a simple gas sensor device, showing clear, high shifts of the reflectance peak that could be easily detected. These high peak shifts are allowed by the ability of the PAVTD technique to produce thin plasma polymer films that exhibit the behaviour of a classical polymer. This property of the films allows expansion of the DBR structure to the levels not attainable with common plasma polymer films.

ACKNOWLEDGEMENTS

This work was supported by the grants GA22-21007S of the Czech Science Foundation and GAUK 411822 of the Charles University Grant Agency.

REFERENCES

[1] ZADEHNAZARI, A. Metal oxide/polymer nanocomposites: A review on recent advances in fabrication and applications. *Polymer-Plastics Technology and Materials.* 2022, vol. 62, no. 5, pp. 655–700, Available from: https://doi.org/10.1080/25740881.2022.2129387

[2] CHOUKOUROV, A. and MANGOLINI, L. Special issue: Plasma synthesis of nanoparticles and nanocomposite coatings. *Plasma Processes and Polymers.* 2020, vol. 17, no. 5, 2090003. Available from: https://doi.org/10.1002/ppap.202090003

[3] SNYDERS, R., HEGEMANN, D., THIRY, D., ZABEIDA, O., KLEMBERG-SAPIEHA, J., MARTINU, L. Foundations of plasma enhanced chemical vapor deposition of functional coatings. *Plasma Sources Science and Technology*. 2023, vol. 32, no. 7, 074001. Available from: https://doi.org/10.1088/1361-6595/acdabc

[4] SUN, L., GRANT, J. T., JONES, J. G., MURPHY, N. R., VERNON, J. P., STEVENSON, P. R. Tailoring the Optical Properties of Nanoscale-Thick Metal–Dielectric Ag–SiO2 Nanocomposite Films for Precision Optical Coating Integration. *ACS Applied Nano Materials*. 2023, vol. 6, no. 9, pp. 7704-7714. Available from: https://doi.org/10.1021/acsanm.3c00853

[5] FAUPEL, F., ZAPOROJTCHENKO, V., STRUNSKUS, T., ELBAHRI, M. Metal-Polymer Nanocomposites for Functional Applications. *Advanced Engineering Materials.* 2010, vol. 12, no. 12, pp. 1177-1190. Available from: https://doi.org/10.1002/adem.201000231

[6] WANG, L., KAFSHGARI, M., MEUNIER, M. Optical Properties and Applications of Plasmonic-Metal Nanoparticles. *Advanced Functional Materials.* 2020, vol. 30, no. 51, 2005400. Available from: https://doi.org/10.1002/adfm.202005400

[7] PRAKASH, J., SUN, S., SWART, H., GUPTA, R. Noble metals-TiO2 nanocomposites: From fundamental mechanisms to photocatalysis, surface enhanced Raman scattering and antibacterial applications. *Applied Materials Today.* 2018, vol. 11, pp. 82-135. Available from: https://doi.org/10.1016/j.apmt.2018.02.002

[8] MISRA, S., LI, L., JIAN, J., HUANG, J., WANG, X., ZEMLYANOV, D., JANG, J., RIBEIRO, F., WANG, H. Tailorable Au Nanoparticles Embedded in Epitaxial TiO2 Thin Films for Tunable Optical Properties. *ACS Applied Materials & Interfaces.* 2018, vol. 10, is. 38, pp. 32895-32902. Available from: https://doi.org/10.1021/acsami.8b12210

[9] DRUFFEL, T., MANDZY, N., SUNKARA, M., GRULKE, E. Polymer nanocomposite thin film mirror for the infrared region. *Small.* 2008, vol. 4, no. 4, pp. 459-461. Available from: https://doi.org/10.1002/smll.200700680

[10] SUN, Y., WANG, G., ZHANG, T., LIU, C., WANG, J. Periodically alternated metallic/dielectric nanocomposites and dielectric films for the fabrication of high-efficiency Bragg reflectors: a case study. *Applied Physics Express.* 2020, vol. 13, no. 7, 072001. Available from: https://doi.org/10.35848/1882-0786/ab93e8

[11] QU, L., ZHAO, J., YANG, J., SUN, Y., LIU, C., Influence of the thermal evolution of Au nanoparticles induced by ion implantation on the reflectivity of multilayer structures. *Optical Materials Express.* 2021, vol. 11, no. 4, pp. 1176-1184. Available from: https://doi.org/10.1364/OME.419456

[12] FAUPEL, F., ZAPOROJTCHENKO, V., GREVE, H., SCHÜRMANN, U., CHAKRAVADHANULA, V.S.K., HANISCH, C., KULKARNI, A., GERBER, A., QUANDT, E. and PODSCHUN, R. Deposition of Nanocomposites by Plasmas. *Contributions to Plasma Physics*. 2007, vol. 47, no. 7, pp. 537-544. Available from: https://doi.org/10.1002/ctpp.200710069

[13] KYLIÁN, O., NIKITIN, D., HANUŠ, J., ALI-OGLY, S., PLESKUNOV, P., BIEDERMAN, H. Plasma-assisted gas-phase aggregation of clusters for functional nanomaterials. *Journal of Vacuum Science & Technology A.* 2023, vol. 41, no. 2, 020802. Available from: https://doi.org/10.1116/6.0002374

[14] KRTOUŠ, Z., KOUSAL, J., SEDLAŘÍKOVÁ, J., KOLÁŘOVÁ RAŠKOVÁ, Z., KUČEROVÁ, L., KRAKOVSKÝ, I., KUČERA, J., ALI-OGLY, S., PLESKUNOV, P., CHOUKOUROV, A. Thin films of crosslinked polylactic acid as tailored platforms for controlled drug release. *Surface and Coatings Technology.* 2021, vol. 421, 127402. Available from: https://doi.org/10.1016/j.surfcoat.2021.127402

[15] KOUSAL, J., KRTOUŠ, Z., SOLAŘ, P., KŘIVKA, I., KRAKOVSKÝ, I., Plasma-assisted vapour thermal deposition with continuous material feed. In: *Proceedings of 14th Nanocon 2022.* Brno: Tanger, 2023, pp. 261-266. ISSN: 2694-930X. Available from: https://doi.org/10.37904/nanocon.2022.4579

[16] CONVERTINO, A., CAPOBIANCHI, A., VALENTINI, A. and CIRILLO, E.N.M. A New Approach to Organic Solvent Detection: High-Reflectivity Bragg Reflectors Based on a Gold Nanoparticle/Teflon-like Composite Material. *Advanced Materials.* 2003, vol. 15, no. 13, pp. 1103-1105, Available from: https://doi.org/10.1002/adma.200304777

[17] JALKANEN, T., TORRES-COSTA, V., SALONEN, J., BJÖRKQVIST, M., MÄKILÄ, E., MARTÍNEZ-DUART, J.M., LEHTO, V.-P. Optical gas sensing properties of thermally hydrocarbonized porous silicon Bragg reflectors. *Optics Express.* 2009, vol. 17, no. 7, pp. 5446-5456. Available from: https://doi.org/10.1364/oe.17.005446

[18] LOVA, P., MANFREDI, G., BOARINO, L., COMITE, A., LAUS, M., PATRINI, M., MARABELLI, F., SOCI, C., COMORETTO, D. Polymer Distributed Bragg Reflectors for Vapor Sensing. *ACS Photonics.* 2015, vol. 2, no.4, pp. 537−543. Available from: https://doi.org/10.1021/ph500461w

[19] KOU, D., ZHANG, Y., ZHANG, S., WU, S., MA, W. High-sensitive and stable photonic crystal sensors for visual detection and discrimination of volatile aromatic hydrocarbon vapors. *Chemical Engineering Journal.* 2019, vol. 375, 121987. Available from: https://doi.org/10.1016/j.cej.2019.121987

[20] PALO, E., DASKALAKIS. K.S., Prospects in Broadening the Application of Planar Solution-Based Distributed Bragg Reflectors. *Advanced Materials Interfaces.* 2023, vol. 10, no. 19, 2202206. Available from: https://doi.org/10.1002/admi.202202206

[21] WEI, J., YI, Z., YANG, L., ZHANG, L., YANG, J., QIN, M., CAO, S. Photonic crystal gas sensors based on metal–organic frameworks and polymers. *Analytical Methods.* 2024, vol 16, no. 29, pp. 4901-4916. Available from: https://doi.org/10.1039/D4AY00764F